Some phonon effects in $S(\mathbf{q})$ for bcc metals

A. M. Rosenfeld
Alcan International Ltd., Kingston Research and Development Centre, P.O. Box 8400, Kingston, Ontario, Canada K7L 5L9

M. J. Stott
Department of Physics, Queen's University, Kingston, Ontario, Canada K7L 3N6
(Received 9 March 1990; revised manuscript received 25 June 1990)

The static structure factor $S(\mathbf{q})$ of solid bcc metals is investigated within the harmonic lattice approximation. Fine structure found in the diffuse background of $S(\mathbf{q})$ is studied for the alkali metals and for Nb and Mo using realistic force constants that are consistent with observed phonon spectra. Ancillary peaks in $S(\mathbf{q})$ between Bragg peaks previously found for Li and Na along high-symmetry directions in $\mathbf{q}$ space are shown to result from extended structure in $S(\mathbf{q})$. These well-defined features that extend from Bragg peaks, and in some cases span them, are readily accounted for in terms of the frequencies and polarizations of the phonons. These features are in turn related to particular lattice deformations that occur in common phase transformations of the bcc lattice. A relationship is noted between the calculated structure and similar features observed in neutron- and x-ray-scattering studies of the martensitic transformation in the alkali metals, charge-density waves in K, and the ω phase in Zr-Nb alloys.

I. INTRODUCTION

Our study of the resistivity change on melting for simple metals based on the difference in $S(\mathbf{q})$, the static structure factor, between the liquid and crystalline solid[1] led us to a direct calculation of $S(\mathbf{q})$ for hot solid potassium. During the course of the work on K, a series of prominent peaks away from Bragg positions was found in $S(\mathbf{q})$ along particular directions in reciprocal space. Similar structure had, in fact, been found earlier by Straus and Ashcroft[2] in a study of the thermal diffuse x-ray scattering in alkali metals. The structure was incidental to the aim of their work although some comments were provided suggesting the generality of the phenomenon. The existence of this dynamical structure has recently been reemphasized by Ashcroft[3] as a possible factor in structural studies based on total-energy calculations. However, a thorough exploration of such effects in reciprocal space and for different metals has yet to be carried out.

In view of the considerable current interest in the lattice dynamics and structural phase transformations of bcc metals, we believe that this calculated structure in $S(\mathbf{q})$ deserves to be more widely recognized and investigated. This is particularly so in the alkali metals where there is interest in martensitic phase transformations in Li[4], Na[5–7], and Rb[8], and in charge-density waves in K.[9–13] The bcc transition metals have also enjoyed attention recently due to the rather pronounced features[14] and anomalously low-lying branches[15,16] observed in the phonon spectra of some of these metals.

Accordingly, we investigate here the calculated peak structure by surveying $S(\mathbf{q})$ in some detail for the alkali metals; we also make some preliminary explorations of the bcc transition metals Nb and Mo. We find that the calculated structure in $S(\mathbf{q})$ for these metals fall into quite specific classes and can be ascribed to characteristic features of the phonon dispersion. These, in turn, can be related to particular lattice distortions that may occur in common phase transformations of the bcc lattice. It emerges that particular behavior associated with precursor effects to phase transformations in many bcc alloys, which is manifested as fine structure in the diffuse scattering contribution to $S(\mathbf{q})$, is already present, to some extent, in the harmonic lattice dynamics of elemental bcc metals. That these effects have not been recognized before in the alkali metals, for example, is not particularly surprising in view of the rather localized surveys of reciprocal space that have been carried out in searching at high resolution for specific peaks associated with the $9R$ martensite or charge-density-wave structures. Nevertheless, there appears to be evidence already for the calculated structure in the form of unexplained anomalies in the diffuse scattering observed for K.

In Sec. II we briefly outline the calculation of $S(\mathbf{q})$. Section III focuses on the alkali metals. We first exhibit representative examples of the peak structure initially observed and a tentative correlation of this structure with inherent instabilities of the bcc lattice towards particular phase transitions is proposed. A more extensive two-dimensional survey of $S(\mathbf{q})$ is then described revealing more extended structure than that found previously.[2] The relationship of this structure to martensitic phase transformations such as those which actually occur in the alkali metals is then examined. In Sec. IV, the survey of $S(\mathbf{q})$ is repeated for Nb and Mo and the additional structure found is discussed in terms of the phase transformation of the bcc lattice to the ω structure. Section V discusses the role of $S(\mathbf{q})$ in signaling lattice instabilities, and notes the differing transformation tendencies of the alkali and bcc transition metals already evident in their harmonic dynamics.

 ©1990 The American Physical Society

II. CALCULATION OF $S(\mathbf{q})$

The static structure factor for finite $\mathbf{q}$ is given by

$$S(\mathbf{q})=N^{-1}\langle n_{\mathbf{q}}n_{-\mathbf{q}}\rangle=N^{-1}\sum_{i,j}\langle\exp[i\mathbf{q}\cdot(\mathbf{R}_i-\mathbf{R}_j)]\rangle, \tag{1}$$

where $n_{\mathbf{q}}$ is the ion density operator, N the total number of ions, $\mathbf{R}_i$ the ion coordinates, and the expectation value denotes a configuration average. The closed form expression of $S(\mathbf{q})$ for a crystalline metal within the harmonic approximation has been known for some time.[17] With $\mathbf{u}_j$ the displacements of the ions from their equilibrium positions $\mathbf{R}_j^0$, and in terms of the displacement correlation functions $\Lambda_{\alpha\beta}(R_{ij}^0)=2\langle u_{i\alpha}u_{j\beta}\rangle$ and the auto-correlation function $\Lambda_{\alpha\beta}(0)=2\delta_{\alpha\beta}\langle|\mathbf{u}_i|^2\rangle/3=\delta_{\alpha\beta}\Lambda_0$, which is diagonal for cubic symmetry, $S(\mathbf{q})$ can be written as

$$S(\mathbf{q})=\exp(-\tfrac{1}{2}q^2\Lambda_0)\sum_j\exp(i\mathbf{q}\cdot\mathbf{R}_j^0)\exp[\tfrac{1}{2}q_\alpha q_\beta\Lambda_{\alpha\beta}(\mathbf{R}_j^0)]\ , \tag{2}$$

where

$$\overleftrightarrow{\Lambda}(\mathbf{R}_j)=(\hbar/MN)\sum_{\mathbf{k},\lambda}\mathbf{e}_{\mathbf{k}\lambda}\mathbf{e}_{\mathbf{k}\lambda}\omega_{\mathbf{k}\lambda}^{-1}\coth(\tfrac{1}{2}\beta\hbar\omega_{\mathbf{k}\lambda})\cos(\mathbf{k}\cdot\mathbf{R}_j^0)\ ,$$
$$\Lambda_0=(\hbar/3MN)\sum_{\mathbf{k},\lambda}\omega_{\mathbf{k}\lambda}^{-1}\coth(\tfrac{1}{2}\beta\hbar\omega_{\mathbf{k}\lambda})\ . \tag{3}$$

In Eqs. (2) and (3), $\omega_{\mathbf{k}\lambda}$ and $\mathbf{e}_{\mathbf{k}\lambda}$ are the frequency and polarization vector of the phonon with wave vector $\mathbf{k}$ and mode index λ, M is the ion mass, $\beta=1/k_BT$, and the $\mathbf{k}$ sum extends over the first Brillouin zone. The constant Λ_0 is related to the familiar Debye-Waller factor $\exp[-2W(q)]$ by $2W(q)=\frac{1}{2}q^2\Lambda_0$.

In performing the calculations we partition $S(\mathbf{q})$ into one-phonon and multiphonon parts and use an approximation for the latter given by Straus and Ashcroft.[2] The temperature-dependent quantity Λ_0 was evaluated directly from Eq. (3) using a simple cubic mesh of wave vectors in the irreducible $\frac{1}{48}$ portion of the Brillouin zone[18] with $\omega_{\mathbf{k}\lambda}$ and $\mathbf{e}_{\mathbf{k}\lambda}$ determined at each point by diagonalizing the dynamical matrix.

Dynamical matrices used in these computations were reconstructed from tabulated force constants fitted to the experimental phonon spectra for each of the elements of interest; these are available for all the alkali metals and for both Nb and Mo. It has been demonstrated that force constants derived from phonon data along symmetry directions can lead to spurious features in the predicted off-symmetry behavior.[19] We have verified that the structure of interest is reproduced by different force-constant sets derived from independent experiments and from measurements at different temperatures where these are available, and in the case of Na and K, with force constants derived from an accurate representation of the interatomic potential given by pseudopotential theory.[18] For the results presented here, we have used the force constants of Dolling and Meyer[20] for K and of Powell *et al.*[21] for Nb and Mo.

III. RESULTS FOR ALKALI METALS

A. One-dimensional q scans

We consider first the structure in $S(\mathbf{q})$ along rays joining principal reciprocal lattice points. Within the unit cell of the bcc reciprocal lattice (see Fig. 7), three distinct classes of peaks are found. Along [111], we find a double-peak structure between Bragg positions with maxima located at $\frac{2}{3}(1,1,1)$ and $\frac{4}{3}(1,1,1)$, while along [112] there is a single peak centered at the N point (0.5,0.5,1) (all $\mathbf{q}$ vectors are quoted in units of $2\pi/a$, where a is the lattice constant.) These peaks are illustrated for K at the Debye temperature (100 K) in Figs. 1 and 2, respectively. In the [310] direction, we find an additional single-peak structure between Bragg points centered at (1.5,0.5,0), which is similar in structure to that shown in Fig. 2. The [111] and [310] structures are those first exhibited by Straus and Ashcroft[2] for Li and Na. Similar behavior is seen along other equivalent directions in the unit cell. Beyond the unit cell, a sequence of maxima between successive Bragg peaks is found along the directions given, as well as multiple-peak structures along other reciprocal lattice vectors according to their composition in terms of unit vectors, e.g., at $\frac{1}{3}$, $\frac{1}{2}$, and $\frac{2}{3}$ (5,5,2). As pointed out by Straus and Ashcroft[2] these peaks are undoubtedly related to the so-called "extra spot" structure seen for one-dimensional q scans in early x-ray work.[22]

These peaks are due mainly to the one-phonon term in $S(\mathbf{q})$. The intensities of the peaks increase as a function

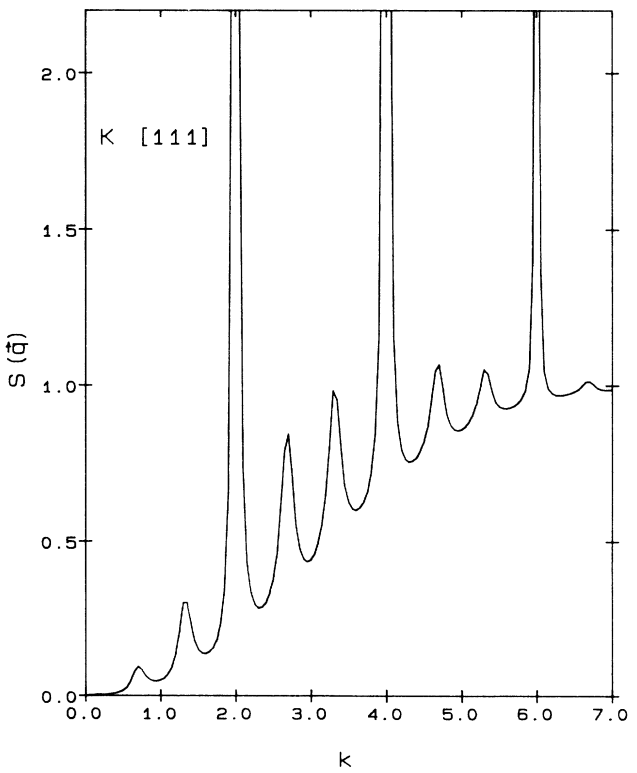

FIG. 1. One-dimensional scan of the structure factor $S(\mathbf{q})$ for potassium at 100 K along [111] with $\mathbf{q}=k(1,1,1)$.

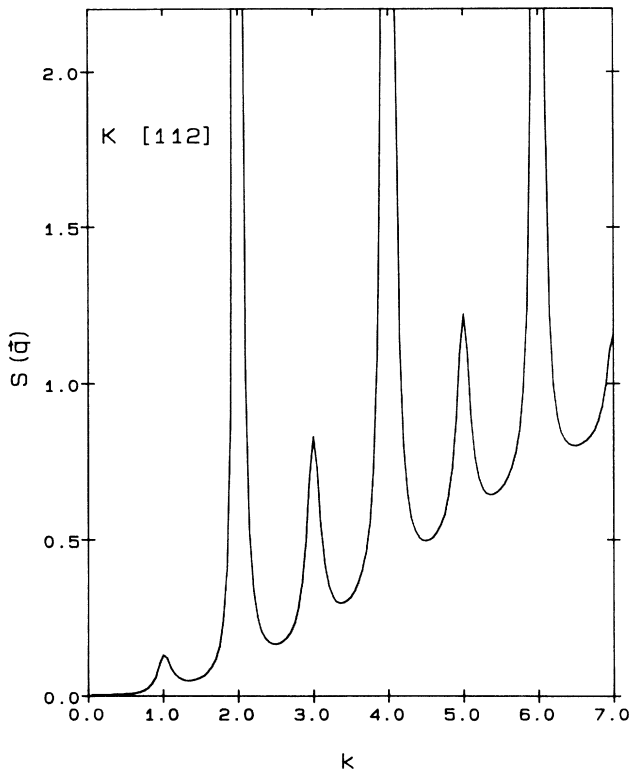

FIG. 2. One-dimensional scan of the structure factor $S(\mathbf{q})$ for potassium at 100 K along [112] with $\mathbf{q}=0.5k(1,1,2)$.

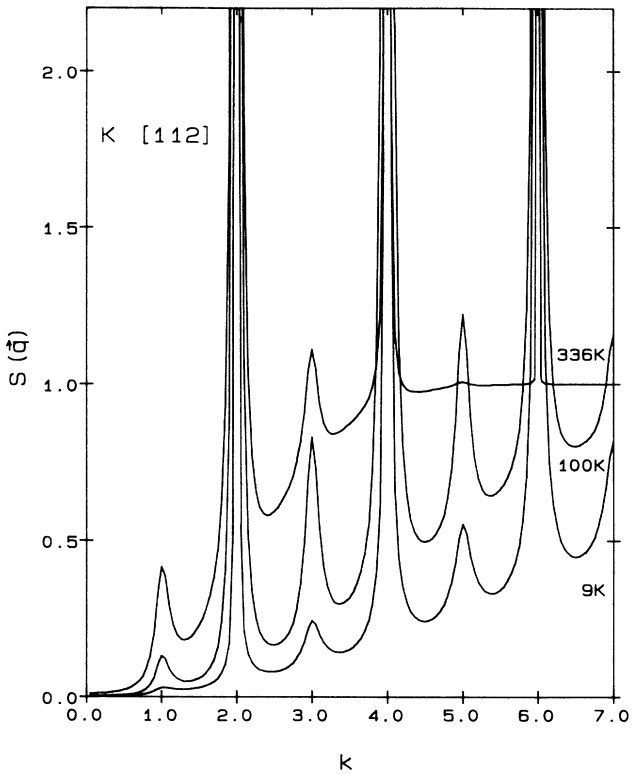

FIG. 3. One-dimensional scan of the structure factor $S(\mathbf{q})$ for potassium along [112] with $\mathbf{q}=0.5k(1,1,2)$ at 9, 100 (Debye temperature) and 336 K (melting point).

of q along a given direction until $S(\mathbf{q})$ is diminished by the Debye-Waller factor. The peaks show a strong temperature dependence (Fig. 3) due to the Debye-Waller effect analogous to that of the diffuse skirts around the Bragg peaks. We find similar structure in all the alkali metals; slight differences in intensity between the peaks found for different elements at equal T/T_M are consistent with deviations from scaling in the phonon spectra.[23]

These peaks between Bragg positions were associated by Straus and Ashcroft[2] with the structure that would be generated quite generally on traversing obliquely the broad valleys separating Bragg points in the function $\omega_{\mathbf{k}\lambda}^{-1}$ which enters the one-phonon term in $S(\mathbf{q})$. Such structure would be found even in a Debye model. Similar behavior was then predicted[2] along any direction except $\langle 100\rangle$ and $\langle 110\rangle$. It was also proposed that features in $S(\mathbf{q})$ would generally result from specific relatively low-lying phonon modes which have the appropriate polarization to be weighted heavily in the sum over modes in Eq. (5). For example the peak at (1.5,0.5,0) in the [310] scan was attributed[2] to the equivalent phonon at the point $N(0.5,0.5,0)$ on the boundary of the first Brillouin zone; the low-lying nature of this transverse zone-boundary phonon along $\langle 110\rangle$ is a well-known characteristic of the alkali metals.[20]

If this proposal were to be taken further then the two remaining peak structures described above could also be associated with two of the other characteristic features of phonon dispersion in the alkali metals, namely, the pronounced dip in the longitudinal mode along [111] at the point $\frac{2}{3}(1,1,1)$ and the minimum at the point (0.5,0.5,1) seen in the phonon spectra[20] along the symmetry axes $(0.5,0.5,\xi)$ and $(\xi,\xi,1)$; this point is also equivalent to N.

We have noted further that the specific phonon modes which could be associated with the calculated peak structures also give rise to atomic displacements that may be obtained in two of the prominent phase transformations of the bcc lattice. It has long been recognized[24] that the dip at the point $\frac{2}{3}(1,1,1)$ is associated with the intrinsic lattice instability of bcc metals towards the ω phase, observed in alloys of Ti, Zr, and Hf with other transition metals. In this transformation, the $\{111\}$ planes of the bcc lattice move such that adjacent planes collapse to the midplane, while every third plane remains unshifted. This corresponds to the condensation of a longitudinal phonon with wave vector $\mathbf{q}=\frac{2}{3}[111]$ and amplitude $a/6$. The resulting additional superlattice reflections of the two layered hexagonal ω structure occur at $\frac{2}{3}$ and $\frac{4}{3}(1,1,1)$ corresponding to the tripling of the unit cell along this direction in real space and coincide with the dynamical structure along [111] illustrated in Fig. 1. Similarly, the bcc to hcp martensitic transformation involves a zone-boundary shear of alternate $\{110\}$ planes parallel to a $\langle 1\bar{1}0\rangle$ direction in these planes[25] which can be mediated by the transverse N point phonon. This suggests that the calculated peaks might be interpreted as incipient Bragg peaks associated with the tendency of the alkali metals to transform structurally. It is thus of some interest to probe the character of the calculated struc-

tures beyond one dimension and elucidate their precise relationship to the underlying phonon dispersion.

B. Two-dimensional survey

In this section we extend our survey of reciprocal space by calculating $S(\mathbf{q})$ over various planes. We begin with the $(1\bar{1}0)$ plane which contains the [111] and [112] directions discussed in the preceding section. Figure 4 shows a contour plot of $S(\mathbf{q})$ for K in this plane between the (1,1,0) and (2,2,0) Bragg positions (we consider a region away from the origin where the intensity is appreciable). The structure factor is dominated by two features, namely, a well-defined ridge, which at the Debye temperature, spans the (1,1,2) and (2,2,0) Bragg peaks along $[1\bar{1}2]$, and at the midpoint of this ridge, a peak at (1.5,1.5,1) equivalent to that at $N(0.5,0.5,1)$ seen in the previous one-dimensional scan along [112]. It is immediately apparent that the peak noted in the previous one-dimensional scan along [111] at the point $\frac{4}{3}[1,1,1)$ arises simply from traversing this ridge and that this point has no special significance; any $\mathbf{q}$ scan cutting this ridge obliquely will exhibit such a peak. On the other hand, the peak at (1.5,1.5,1) is seen to have at least two-dimensional character. The ridge structure found in the $(1\bar{1}0)$ plane is illustrated by the three-dimensional plot in Fig. 5(a). The accompanying Fig. 5(b) is a corresponding plot for the (001) plane; a pronounced ridge is revealed along $[1\bar{1}0]$,

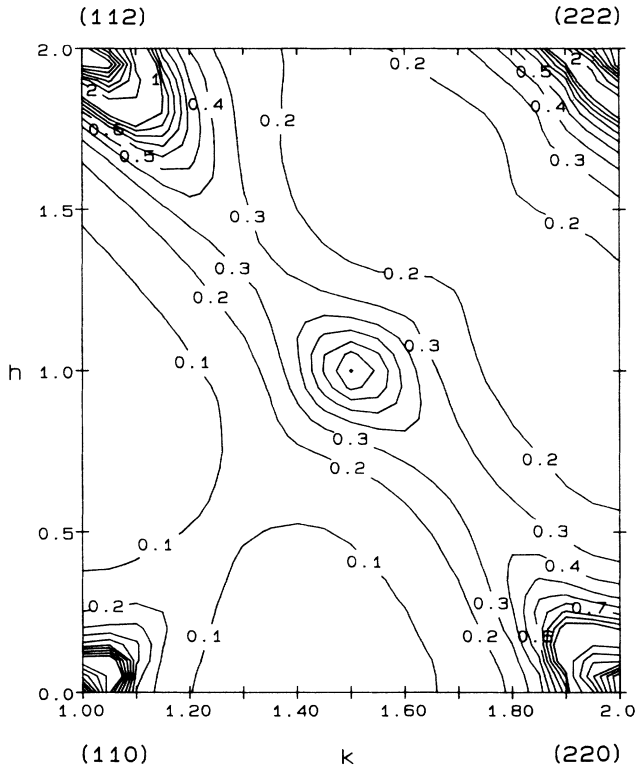

FIG. 4. Contour plot of the structure factor $S(\mathbf{q})$ for potassium at 100 K in the $(1\bar{1}0)$ plane with $\mathbf{q}=(k,k,h)$. (Note that the spacing between contours is incremented at the level equal to 1.0 near the Bragg positions.) The Bragg peaks at the corners are labeled for easy cross reference with Fig. 7.

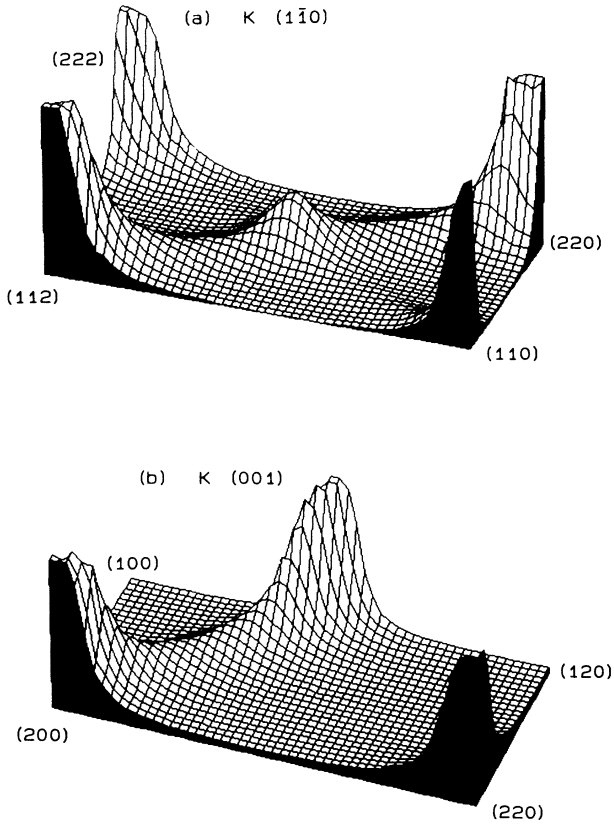

FIG. 5. Three-dimensional plots of the structure factor $S(\mathbf{q})$ for potassium at 100 K in (a) the $(1\bar{1}0)$ plane and (b) the (001) plane.

through the (1,1,0) Bragg point, which spans adjacent Bragg peaks in this direction. The peak noted earlier at (1.5,0.5,0) in the one-dimensional scan along [310] again results simply from cutting this ridge obliquely. These ridges between the Bragg peaks persist down to very low temperature as evidenced by the presence of the (0.5,0.5,1) peak at 9 K in the one-dimensional scan along [112] shown in Fig. 3.

A survey of $\{001\}$ planes reveals structure in $\langle 110\rangle$ directions through every Bragg point. This structure consists of streaks which in some cases appear as ridges spanning adjacent Bragg peaks as in Fig. 5(b), while in other cases these appear as elongations of the diffuse skirts around the Bragg peaks. Figure 6 illustrates both varieties in a (100) plane. Both types of structure were observed in early x-ray photographs[26] for a number of compounds and elements including Na, in particular. The structure near the Bragg peaks was explained[26] in terms of anisotropy in elastic constants while the more extended streaks could not, at that time, be accounted for. The calculated structure in $\langle 110\rangle$ directions at representative (1,1,0) and (1,1,2) points is shown schematically in Fig. 7. A similar survey of $\{1\bar{1}0\}$ planes yields analogous structure along $\langle 112\rangle$ directions through every Bragg point of which one example is the ridge in Fig. 5(a); the latter is also depicted in Fig. 7. We find that streaking is absent at the origin, selected streak absences

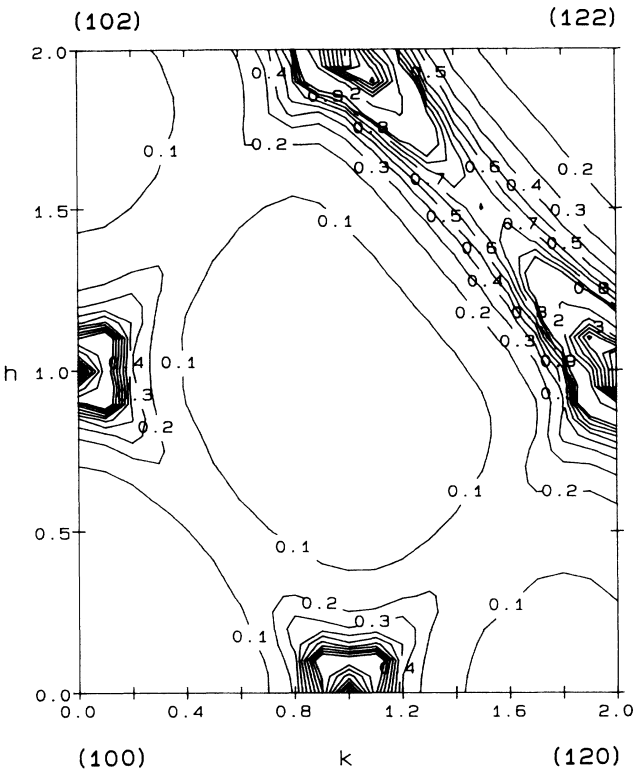

FIG. 6. Contour plot of the structure factor $S(\mathbf{q})$ for potassium at 100 K in the (100) plane with $\mathbf{q}=(1,k,h)$. (Note that the spacing between contours is incremented at the level equal to 1.0 near the Bragg positions.)

out of the 6 ⟨110⟩ or 12 ⟨112⟩ orientations occur systematically at each Bragg point, there is a distribution of intensity for streaks of both types at a given point and the intensity of streaks in a given direction increases with increasing order of Bragg peak.

The prominent peak at (1.5,1.5,1) in Figs. 4 and 5(a) is now seen to result from the intersection of an extended streak of ⟨110⟩ type with another of ⟨112⟩ type (Fig. 7). The height of this peak in the $(1\bar{1}0)$ plane [Fig. 5(a)] affords an indication of the greater intensity of the ⟨110⟩ type streak relative to the ⟨112⟩ type.

Thus we find that the peaks apparent in the structure factor of the alkali metals along particular one-dimensional q scans in reciprocal space can, in all cases, be ascribed to traversing extended structure in $S(\mathbf{q})$. The extended nature of this structure suggests that it is not due to any localized feature in the phonon spectrum such as an anomalously low-frequency phonon. Moreover, the highly anisotropic nature of the structure revealed by a broad survey of reciprocal space cannot be accounted for by the model previously proposed[2] and described above.

C. Interpretation

The origin of the extended streaks in both the $(1\bar{1}0)$ and (001) planes can be explained in terms of the phonon spectra when polarization information is taken into account. We consider, for example, the region of the $(1\bar{1}0)$ plane covered by the contour plot in Fig. 4. The dispersion curves along the two diagonals of this region, i.e., [112] and $[11\bar{2}]$, are shown in Fig. 8 for the two modes with polarization in the plane. These two modes are neither purely transverse nor longitudinal and both will con-

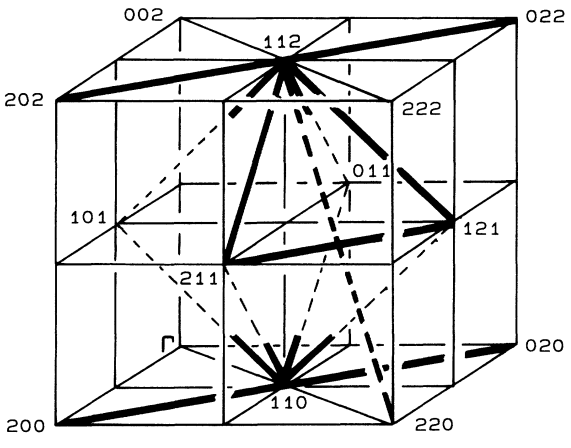

FIG. 7. Schematic of ⟨110⟩ streak structures for potassium through representative points (1,1,0) and (1,1,2). Long and dashed heavy lines correspond, respectively, to streaks spanning Bragg positions or appearing as elongations of Bragg skirts. The dashed heavy line is a streak of ⟨112⟩ type.

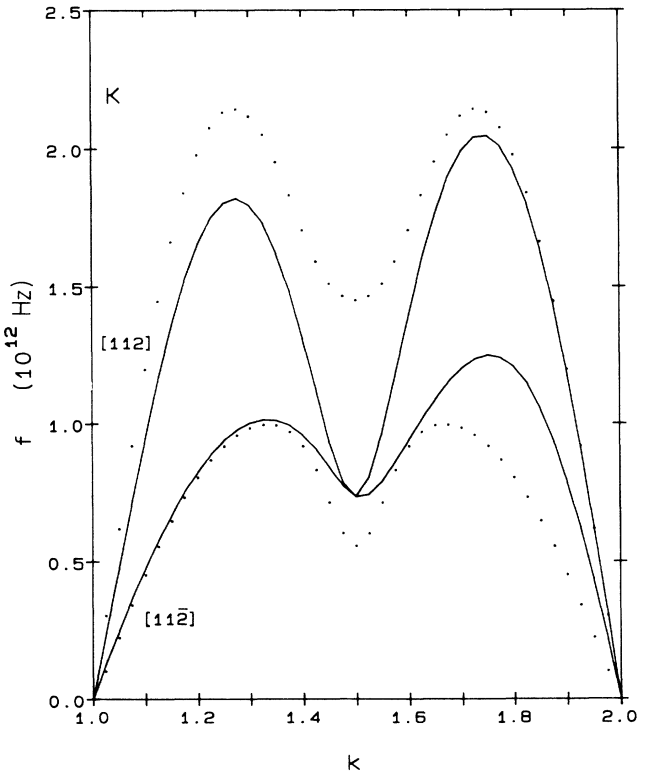

FIG. 8. Phonon-dispersion curves for potassium along ⟨112⟩ directions in the $(1\bar{1}0)$ plane. The dotted curves show the frequencies of the two modes with polarization in the plane. The solid curves show the sum of the frequencies weighted by $|\mathbf{q}\cdot\varepsilon_q|^2$, with $\mathbf{q}=(k,k,2k-2)$ for the [112] direction and $\mathbf{q}=(k,k,4-2k)$ for the $[11\bar{2}]$ direction.

tribute to $S(\mathbf{q})$ along each diagonal; the third mode polarized out of the plane makes no contribution to $S(\mathbf{q})$. The polarization weighted sum of the two in-plane modes is also shown in Fig. 8 for the two directions; this indicates the relative contribution of each mode to $S(\mathbf{q})$ in a given direction. In general, the lowest-lying mode with favorable polarization will make the largest contribution to $S(\mathbf{q})$ due to the reciprocal frequency dependence of the structure factor. Along $[11\bar{2}]$, the polarization weighting selects predominantly the lower phonon branch, and the line of low-lying frequencies is manifest as a ridge parallel to this direction in $S(\mathbf{q})$. Along the transverse [112] direction, however, the upper branch is selected, tending to depress the structure factor in this direction as one moves away from the intersection point at (1.5,1.5,1.0). The definition of the ridge itself is thus due both to the low-lying phonon modes in this direction and to the relatively high modes in the transverse direction.

The ridge structure seen in the (001) plane [Fig. 5(b)] can be similarly accounted for in terms of the two modes polarized in the plane along $\langle 110 \rangle$ directions.

The question thus arises of what is special about the phonon dispersion along $\langle 112 \rangle$ and $\langle 110 \rangle$ directions responsible for the extended streak structures seen in the $(1\bar{1}0)$ and (001) planes. A sound velocity contour analysis, following Miller and Musgrave[27] does yield a pronounced minimum in the velocity surface of the alkali metals for transverse waves in these directions. Such an analysis accounts for the streak structure near the Bragg peaks, but cannot explain the extended ridges seen in Fig. 5.

We have noted that the calculated streak structure is similar to that observed in x-ray and neutron studies of a variety of β-phase alloys, such as Ni-Al alloys, that undergo martensitic transformations.[28,29] In these alloys, this so-called "relrod" behavior, observed well above the transition temperature, has been associated[30] with precursor effects involving particular shear strains. It has been generally shown[31] that a lattice strain, represented by a displacement wave of wave vector $\mathbf{k}$ and polarization $\mathbf{e}_\mathbf{k}$, will generate streaks in the diffuse scattering along the direction $\mathbf{k}$ through every Bragg reflection $\mathbf{G}$, with intensity weighted by $\mathbf{e}_\mathbf{k}\cdot\mathbf{G}$; these occur whether the displacements are static or dynamic in origin. We find that two sorts of lattice strain are sufficient to explain both the number and relative intensities of streaks around each reciprocal lattice point. Thus a shear of $(110)\cdot[1\bar{1}0]$ type, i.e., a shear across the (110) plane in the $[1\bar{1}0]$ direction generates a specific number of streaks along $\langle 110 \rangle$ directions at each reciprocal lattice point, for example, three at (2,2,2), four at (2,0,0), and five at (1,1,0) and (1,1,2). The relative intensity of streaks at a given point is determined by the polarization weights and we find, for example, at (1,1,0), one streak of high intensity and four of lower intensity. The resulting pattern accounts for both the extended ridges and Bragg skirt elongations found by the direct calculation of $S(\mathbf{q})$ as depicted in Fig. 7. The second sort of lattice strain is a shear of $(11\bar{2})\cdot[111]$ type, which accounts for the distribution of streaks of $\langle 112 \rangle$ type at each point. We find all twelve streaks present at (2,0,0) and (2,2,2), nine at (1,1,2), and six at (1,1,0), with, for example, three streaks of high intensity and six of low intensity at (1,1,2).

The same $\langle 110 \rangle$ streak pattern found here has been observed in a number of β-phase alloys[30] and, in a few cases, in conjunction with $\langle 112 \rangle$ streaks.[32] The connection of both types of shear to the bcc to martensite phase transformation in these alloys is known.[35] An appropriate shear of $\{110\}$ planes parallel to a $[1\bar{1}0]$ direction in these planes is required to convert the $ABAB$ bcc stacking to the correct stacking sequence in the martensite while a long-wavelength shear applied to each $\{112\}$ plane, parallel to a [111] direction lying in this plane, is required to convert the trigonal net in the bcc $\{110\}$ planes to hexagonal close packing. Whether the calculated structure can, in fact, be associated with structural transformations in the alkali metals is examined below. We turn next, though, to a brief consideration of elemental transition metals.

IV. RESULTS FOR Nb AND Mo

The element of most direct interest among the bcc transition metal is Zr which undergoes a transition from bcc to hcp at 1135 K; this can be suppressed, however, in favor of a transformation to the ω phase through pressure or alloying. While the phonon dispersion in the high-temperature bcc phase has been measured,[33,34] the sharp dip found in the longitudinal [111] branch and the low-lying [110] branch preclude a meaningful analysis in terms of a harmonic lattice model with a small number of force constants.[35] Accordingly, we focus on Nb and Mo, the neighboring elements in the row, to see whether any systematic development of structure in $S(\mathbf{q})$ can be identified. These elements do show a progression in the depth of the $L\frac{2}{3}[111]$ phonon from Mo through Nb to Zr which has been correlated[36] with the decreasing number of valence electrons in the same sequence.

Figures 9 and 10 show one-dimensional $\mathbf{q}$ scans from the origin of reciprocal space in the [111] and [112] directions for Nb and Mo, respectively. It is evident that the previously found double-peak structure along [111] is present in Nb but not the single-peak structure along [112], while the opposite situation is obtained in Mo. The two-dimensional surveys of $S(\mathbf{q})$ in the $(1\bar{1}0)$ plane, between the (1,1,0) and (2,2,0) Bragg positions, are given in Figs. 11 and 12 respectively. In Nb, a diffuse peak is found near to, but displaced from, the $\frac{4}{3}$ (111) position along the [111] direction with a roughly symmetrical structure present near $(\frac{5}{3},\frac{5}{3},\frac{2}{3})$. The diffuse intensity patterns around these points are elongated in the direction perpendicular to [111], but are shifted to either side of the $[11\bar{2}]$ diagonal and do not link up to form a continuous ridge between the adjacent Bragg peaks as in K. In Mo, a shallow localized maximum is found at the point (1.5,1.5,1). No pronounced streak structure for either metal was found in the (001) plane. Three-dimensional plots of $S(\mathbf{q})$ in the $(1\bar{1}0)$ plane for Nb and Mo are given in Fig. 13.

Unlike the situation in the alkali metals, the peak structure in Nb along [111] arises from traversing a true peak near the Bragg position of the ω phase. With

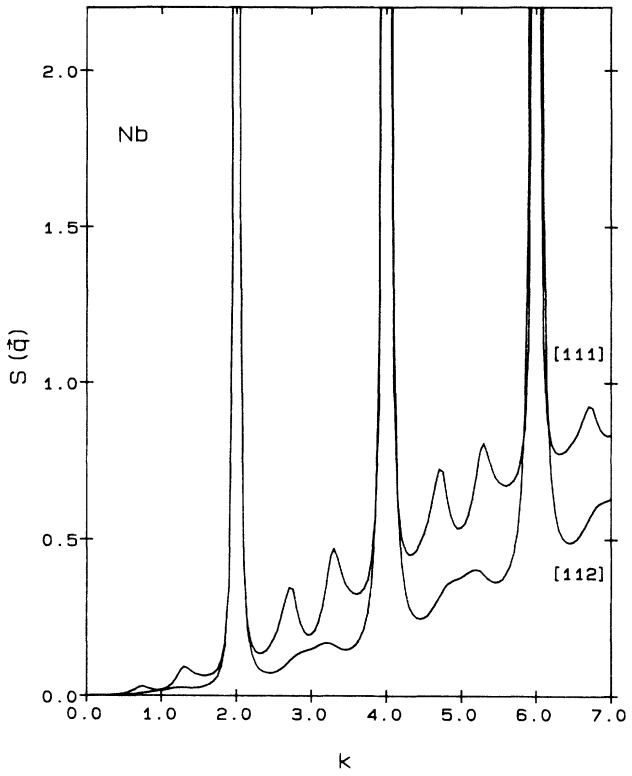

FIG. 9. One-dimensional scan of the structure factor $S(\mathbf{q})$ for Nb at 296 K along [111] with $\mathbf{q}=(1,1,1)$ and along [112] with $\mathbf{q}=0.5k\,(1,1,2)$.

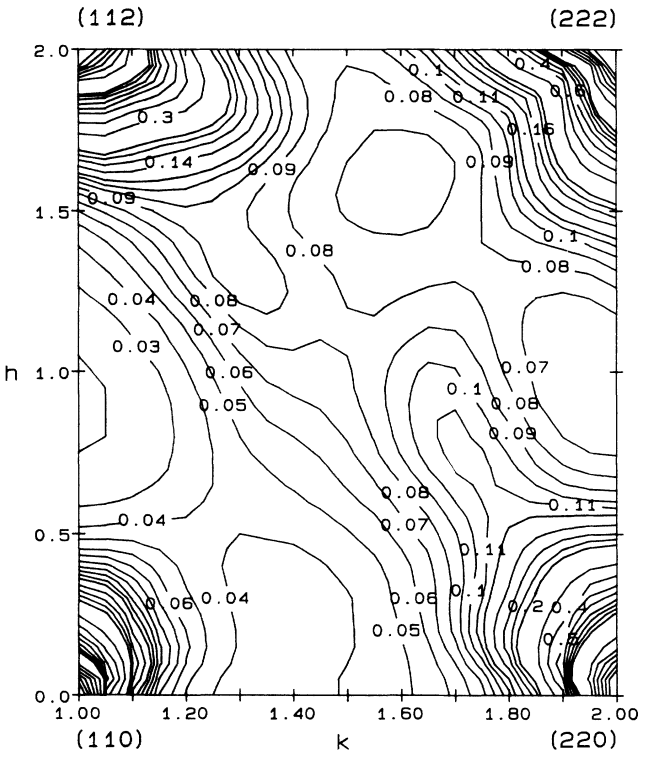

FIG. 11. Contour plot of the structure factor $S(\mathbf{q})$ for Nb at 296 K in the $(1\bar{1}0)$ plane with $\mathbf{q}=(k,k,h)$. (Note that the spacing between levels is incremented at contours equal to 0.12, 0.2, and 1.0 as the Bragg position is approached.)

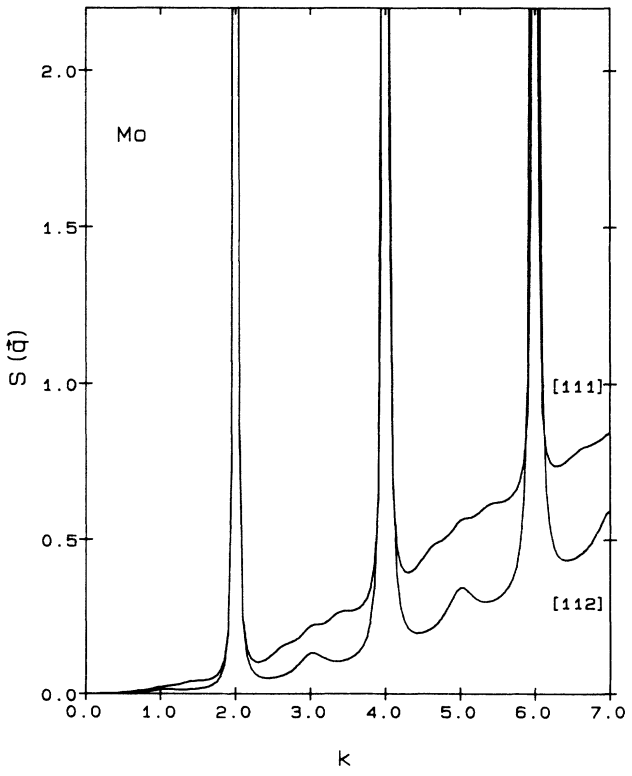

FIG. 10. One-dimensional scan of the structure factor $S(\mathbf{q})$ for Mo at 296 K along [111] with $\mathbf{q}=k(1,1,1)$ and along [112] with $\mathbf{q}=0.5k\,(1,1,2)$.

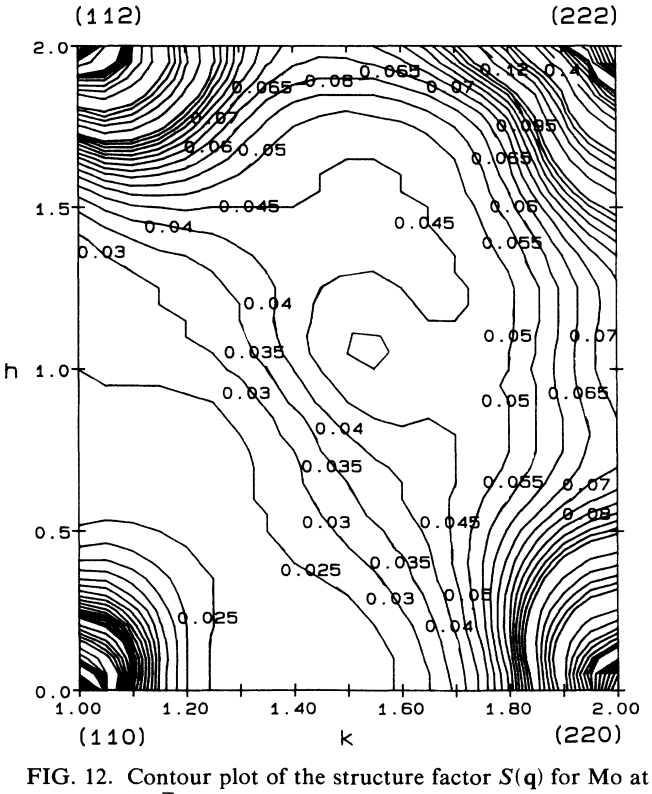

FIG. 12. Contour plot of the structure factor $S(\mathbf{q})$ for Mo at 296 K in the $(1\bar{1}0)$ plane with $\mathbf{q}=(k,k,h)$. (Note that the spacing between contours is incremented at levels equal to 0.12, 0.2, and 1.0 as the Bragg position is approached.)

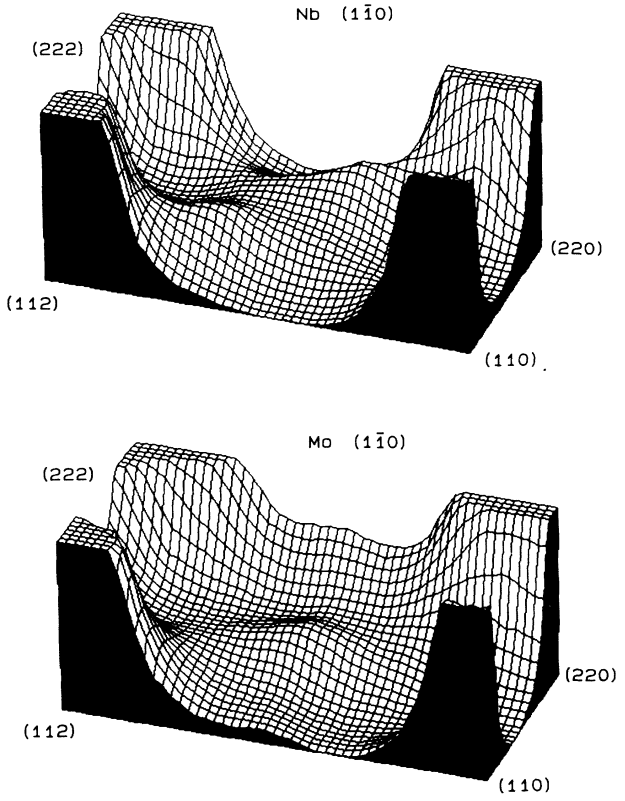

FIG. 13. Three-dimensional plots of the structure factor $S(\mathbf{q})$ for Nb and Mo at 296 K in the (1$\bar{1}$0) plane.

respect to the phonon frequencies, this position is not a saddle point but an absolute minimum, as has been recognized previously in Nb.[37] The position (1.5,1.5,1) in Nb is a saddle point in the phonon spectrum, a minimum along [112] but a maximum along [11$\bar{2}$]; this also contrasts with the situation in the alkali metals. In Mo, the peak in $S(\mathbf{q})$ at (1.5,1.5,1.0) arises from an absolute minimum which survives in the phonon spectrum at this point.

As for the alkali metals, the $S(\mathbf{q})$ results for Nb may be considered in light of the extensive data available on transition-metal alloys exhibiting phase transitions, in this case, to the ω phase. The most comprehensive study has been carried out for Zr-Nb alloys, with compositions ranging from 8–30 wt. % Nb, using Mossbauer and x-ray diffuse scattering[38] and neutron scattering.[39] Alloys in the 5–17 wt.% Nb composition range quenched from the bcc phase were found to exhibit sharp, temperature-independent reflections at the Bragg positions of the ω structure; these were attributed to relatively large and long-lived ω-like particles. For the 17–30 wt.% Nb alloys, qualitatively different behavior was found. Some of the interesting features are as follows. (1) The ω-like reflections become increasingly diffuse as the Nb concentration increases (in general, higher Nb concentration tends to suppress the transformation out of the bcc phase). (2) This diffuse scattering tends to elongate perpendicular to [111] directions. (3) The peaks are displaced from the exact ω superlattice positions, and (4) these persist to 1273 K for Zr–20 at.% Nb, i.e., well into the single-phase bcc region. The structure of this diffuse ω phase has been viewed as one in which atoms are displaced only part of the way to the ideal ω positions giving rise to rumpled (111) planes. The elongation of diffuse scattering is taken to signify the presence of rod-shaped ω domains with their long dimension parallel to [111]. Several models have been proposed[40] for the displacement of the diffuse maxima from the exact ω positions with no single mechanism able to account for the magnitude and sign of the peak shifts. The persistent reflections have been attributed to very long-lived dynamic fluctuations between bcc and ω.

The present results show surprisingly that these features are already present, to some extent, in the harmonic dynamics of Nb. The diffuse ω-like peaks are found with extension perpendicular to [111] (Fig. 11), and the calculated shifts of ~ 0.04 $(2\pi/a)$ in the peak positions from the exact ω phase reflections are of the magnitude observed experimentally. Clearly, there is a great deal more[36] to the anomalous dynamical response seen in the Zr alloys, however the behavior present already in the harmonic response constitutes a base line from which additional effects, such as anharmonicity and quasistatic behavior, should be considered. The structure found in Nb, via a simple force-constant model, underscores the need for heuristic models of transition-metal lattice dynamics.

V. DISCUSSION

A rather detailed set of correlations between phase transformations, phonon anomalies, and diffuse scattering features has emerged for a range of β-phase alloys.[29,30] However, the situation in the alkali metals is not nearly so clear. The lack of any prominent precursor behavior to the martensitic phase transformation in the phonon spectra[5] or elastic constant behavior[6] leaves open the question of the dynamical mechanism of the transformation and of the relevant features that distinguish the different alkali metals in their propensity to transform. In this situation, it appears likely that the characteristics of the transformation may be manifest only in subtle changes or differences in the dynamical behavior. These may be more apparent in the diffuse scattering in $S(\mathbf{q})$ which is sensitive to the polarization of the displacement waves and hence the competition between waves corresponding to different sets of displacements. Anomalous behavior in the diffuse scattering in the alkali metals has been recently reported in Li[4], Na[5], and K.[13] In Li and Na, diffuse scattering was observed in radial scans near the [1$\bar{1}$0] direction which was attributed to point defects. In Li, additional streaking between (1,1,0) and (2,2,0) Bragg reflections was found and ascribed to planar defects related to the bcc-martensitic transformation, such as stacking faults parallel to {110} planes. However, this interpretation is not consistent with the conventional analysis used here which would point rather to nonradial streaks if {110}·[1$\bar{1}$0] shears are involved. In K, temperature-dependent and asymmetric structure was seen close to the (1,1,0) and (2,2,0) Bragg reflections and ascribed to Huang scattering due to defect formation. These experiments considered only radial scans and thus were not sensitive to the extended streak structure calcu-

lated here. More detailed experiments are encouraged.

We observe also that the streaks around the Bragg points shown in Fig. 6 and schematically in Fig. 7, will lead to peaks in $S(\mathbf{q})$ for $\mathbf{q}$ scans in certain directions which pass close to the Bragg peaks. For example, we find for K a double-peak structure for scans along [001] in the $[1\bar{1}0]$ scattering plane near the (110) Bragg point as shown in Fig. 14. These peaks are similar in structure to those observed for the same scans in a recent experimental search for charge-density-wave (CDW) satellites in K.[11] The structure found here arises from the projection of a pair of $\langle 110 \rangle$ streaks, one above and the other below the $(1\bar{1}0)$ plane, in analogous manner to that which would arise from CDW satellites located at the predicted positions and having a diffuse phason scattering distribution elongated along [110].[11] Our calculated peak positions for the particular scans studied in that experiment are close to those actually observed and which have been attributed to the CDW. The ratio of satellite to Bragg intensity found experimentally is of order 10^{-5}. This agrees with current theoretical estimates based on CDW models, however, a tight quantitative comparison was not made[11] because the (1,1,0) Bragg peak is reduced by extinction and the CDW model would suggest some reduction of the satellites due to phason scattering. The ratio we calculate here is about an order of magnitude lower than the raw experimental data but we anticipate that there will be sensitivity to variations in the force constants as well as to anharmonic effects that remain to be explored. We also find peaks in the (001) scattering plane near the observed locations for additional experimental features reported in Ref. 11, though these are much less pronounced than the experimental peaks due to the dominating background from the $[1\bar{1}0]$ ridge in this plane (Fig. 7). A calculation of the measurable intensity of these peaks by convoluting $S(\mathbf{q})$ with an appropriate resolution function, would be required to confirm that the sharp features which we find to be present in $S(\mathbf{q})$ for the harmonic lattice can be ruled out as a contributing factor to the observed peak structure attributed to the CDW in Ref. 11.

Some features observed in other CDW searches are unexplained. In one study[10] using x rays, a series of scans carried out with energy resolution low enough to be sensitive to thermal diffuse scattering revealed anomalous peaks which were regarded as spurious and not described in any detail. In their early search for a CDW in K, Werner *et al.*[42] observed a series of peaks along [110] as well as peaks at 0.63(1,1,1) and (0.5,0.5,0.95) which were far from any predicted CDW reflections and for which no explanation could be found. This structure has been consistently overlooked in more recent studies as noted by Wilson and de Podesta,[12] who suggested that the [110] peaks occur near points appropriate to the 9*R* martensite structure and that these provide evidence for an incipient lattice instability in K. We observe that the remaining two peaks are close to those at $\frac{2}{3}(1,1,1)$ and (0.5,0.5,1) shown in the one-dimensional scans in Figs. 1 and 2, arising from the dynamical structure of the harmonic lattice.

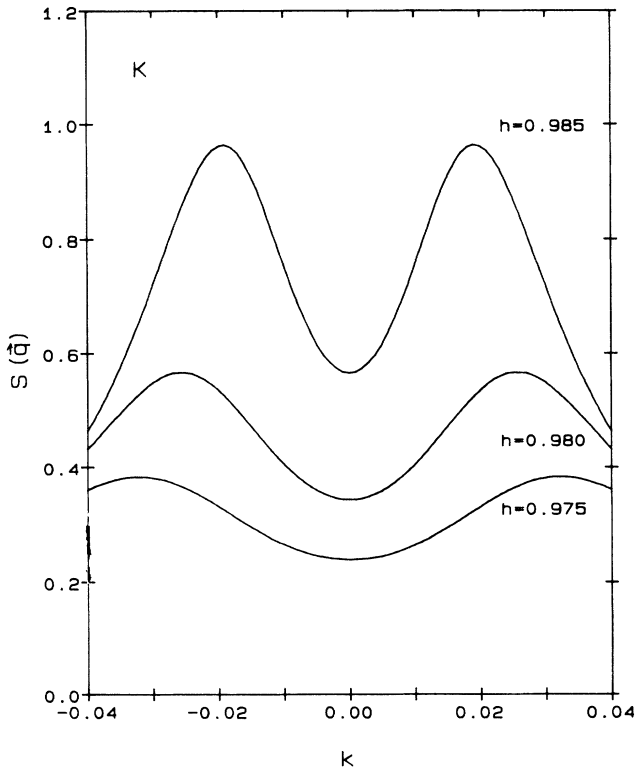

FIG. 14. One-dimensional scan of the structure factor $S(\mathbf{q})$ for potassium at 4.2 K in the [001] direction with $\mathbf{q}=(h,h,k)$, corresponding to Fig. 2 of Ref. 11.

VI. CONCLUSION

In summary, we find that the particular behavior associated with precursor effects to martensitic phase transformations in bcc alloys is already present, to some extent, in the harmonic lattice dynamics of elemental bcc metals. These are manifested as fine structure in the diffuse scattering contribution to $S(\mathbf{q})$. This structure consists, in the alkali metals, of $\langle 110 \rangle$ and $\langle 112 \rangle$ streaks extending as ridges between Bragg positions or as elongations of the Bragg peak skirts. These streaks give rise to apparent peak structures in one-dimensional scans along particular directions in reciprocal space, which may be associated with peaks already seen in searches for CDW satellites in K. Surveys of diffuse scattering in the alkali metals have not been sufficiently broad to reveal the calculated structure. Additional structure was also found in the bcc transitional metals Nb and Mo. In Nb, diffuse peaks are found near the Bragg positions of the ω phase which exhibit several of the characteristics ascribed to quasistatic displacement waves or embryonic behavior in Zr-Nb alloys. Similar structure is also anticipated for bcc Zr and has recently been observed experimentally,[43] but detailed investigation awaits advances in the treatment of the lattice dynamics for this metal. Comparing the results for the transition and alkali metals, it is evident that the propensity to transform either into the ω phase or to martensite is already signaled by the rather different harmonic dynamical behavior in these classes of metals.

As emphasized by Ashcroft,[3] fine structure in $S(\mathbf{q})$ resulting from dynamical effects may influence properties related to the total energy. Our work lays out the extent and origins of such structure for bcc metals. Preliminary results indicate the presence of dynamical fine structure in $S(\mathbf{q})$ for Mg and Zn, and further work exploring $S(\mathbf{q})$ for hcp and other structures would appear to be warranted. The incorporation of anharmonic effects in $S(\mathbf{q})$ is also worthy of investigation.

ACKNOWLEDGMENTS

This work was supported by the Natural Sciences and Engineering Research Council of Canada.

[1]A. M. Rosenfeld and M. J. Stott, Phys. Rev. B **42**, 3406 (1990).
[2]D. M. Straus and N. W. Ashcroft, Phys. Rev. B **14**, 448 (1976).
[3]N. W. Ashcroft, Phys. Rev. B **39**, 10 552 (1989).
[4]G. Ernst, C. Artner, O. Blaschko, and G. Krexner, Phys. Rev. B **33**, 6465 (1986).
[5]O. Blaschko and G. Krexner, Phys. Rev. B **30**, 1667 (1984).
[6]J. Szente and J. Trivisonno, Phys. Rev. B **37**, 8447 (1988).
[7]C. M. McCarthy, C. W. Tompson, and S. A. Werner, Phys. Rev. B **22**, 574 (1980); A. W. Overhauser, Phys. Rev. Lett. **53**, 64 (1984); R. Berliner and S. A. Werner, Phys. Rev. B **34**, 3586 (1986); H. G. Smith, Phys. Rev. Lett. **58**, 1228 (1987).
[8]I. M. Templeton, J. Phys. F **12**, L121 (1982).
[9]L. Pintschovious, O. Blaschko, G. Krexner, M. de Podesta, and R. Currat, Phys. Rev. B **35**, 9330 (1987).
[10]H. You, J. D. Axe, D. Hohlwein, and J. B. Hastings, Phys. Rev. B **35**, 9333 (1987).
[11]T. M. Giebultowicz, A. W. Overhauser, and S. A. Werner, Phys. Rev. Lett. **56**, 1485 (1986).
[12]J. A. Wilson and M. de Podesta, J. Phys. F **16**, L121 (1986).
[13]O. Blaschko, M. de Podesta, and L. Pintschovius, Phys. Rev. B **37**, 4258 (1988).
[14]C. Stassis, in *Methods of Experimental Physics*, Vol. 23 of *Neutron Scattering*, edited by K. Sköld and D. L. Price (Academic, New York, 1986), p. 369.
[15]C. Stassis and J. Zaretsky, Solid State Commun. **52**, 9 (1984).
[16]W. Petry, T. Flottmann, A. Heiming, J. Trampenau, M. Alba, and G. Vogl, Phys. Rev. Lett. **61**, 722 (1988).
[17]A. A. Maradudin, E. W. Montroll, G. H. Weiss, and I. P. Ipatova, in *Solid State Physics*, 2nd ed., edited by H. Ehrenreich, F. Seitz, and D. Turnbull (Academic, New York, 1971).
[18]R. C. Shukla and R. Taylor, J. Phys. F **6**, 531 (1976).
[19]R. Stedman, L. Almqvist, and G. Nilsson, Phys. Rev. **162**, 549 (1967); R. C. Dynes, J. P. Carbotte, and E. J. Woll, Jr., Solid State Commun. **6**, 101 (1968).
[20]G. Dolling and J. Meyer, J. Phys. F **7**, 775 (1977).
[21]B. M. Powell, P. Martel, and A. D. B. Woods, Can. J. Phys. **55**, 1601 (1977).
[22]J. E. Eldridge and T. R. Lomer, Proc. Phys. Soc. **91**, 459 (1967), and other articles cited in Ref. 2.
[23]J. R. D. Copley and B. N. Brockhouse, Can. J. Phys. **51**, 657 (1973).
[24]D. de Fontaine, Acta. Metall. **18**, 275 (1970).
[25]W. G. Burgers, Physica **1**, 561 (1934).
[26]K. Lonsdale, Proc. Phys. Soc. **54**, 314 (1942).
[27]G. F. Miller and M. J. P. Musgrave, Proc. R. Soc. London, Ser. A **236**, 352 (1956).
[28]A. Nagasawa, N. Nakaniski, and K. Enami, Philos. Mag. A **43**, 1345 (1981).
[29]S. M. Shapiro, J. Z. Larese, Y. Noda, S. C. Moss, and L. E. Tanner, Phys. Rev. Lett. **57**, 3199 (1986), and references therein.
[30]L. E. Tanner, A. R. Pelton, and R. Gronsky, J. Phys. (Paris) Colloq. **43**, C4-169 (1982); I. M. Robertson and C. M. Wayman, Philos. Mag. A **48**, 421 (1983); A **48**, 4443 (1983); A **48**, 629 (1983).
[31]A. Guinier, *X-Ray Diffraction* (Freeman, San Francisco, 1963).
[32]K. Enami, J. Hasunuma, A. Nagasawa, and S. Nenno, Scr. Met. **10**, 879 (1976).
[33]C. Stassis, J. Zaretsky, and N. Wakabayaski, Phys. Rev. Lett. **41**, 1726 (1978).
[34]W. Petry, A. Heiming, J. Trampenau, and G. Vogl, *Defect and Diffusion Forum*, edited by F. J. Kedves and D. L. Beke (Sci-Tech, Brookfield, VT, 1990), Vols. 66–69, p. 157.
[35]Y. Chen, C. L. Fu, K.-M. Ho, and B. N. Harmon, Phys. Rev. B **31**, 6775 (1985); F. Willaime and C. Massobrio, Phys. Rev. Lett. **63**, 2244 (1989).
[36]K. M. Ho, C. L. Fu, and B. N. Harmon, Phys. Rev. B **29**, 1575 (1984).
[37]S. C. Moss, J. Phys. (Paris) Colloq. **38**, C7-440 (1977).
[38]W. Lin, H. Spalt, and B. W. Batterman, Phys. Rev. B **13**, 5158 (1976).
[39]S. C. Moss, D. T. Keating, and J. D. Axe, in *Phase Transformations*, edited by L. E. Cross (Pergamon, New York, 1973), p. 179; Y. Noda, Y. Yamada, and S. M. Shapiro, Phys. Rev. B **40**, 5995 (1989).
[40]B. Borie, J. Phys. F **12**, 1285 (1982), and references therein.
[41]A. Nagasawa, J. Phys. Soc. Jpn. **40**, 93 (1976).
[42]S. A. Werner, J. Eckert, and G. Shirane, Phys. Rev. B **21**, 581 (1980).
[43]A. Heiming, W. Petry, J. Trampenau, M. Alba, C. Herzig, and G. Vogl, Phys. Rev. B **40**, 11 425 (1989).